

Experimental Study on Z-Pin Bridging Law by Pullout Test

Shao-Cong Dai^a, Wenyi Yan, Hong-Yuan Liu^{a*} and Yiu-Wing Mai^a

^a*Centre for Advanced Materials Technology (CAMT), School of Aerospace, Mechanical and Mechatronic Engineering J07, The University of Sydney, Sydney, NSW 2006, Australia*

^b*Computational Engineering Research Centre, Faculty of Engineering and Surveying, The University of Southern Queensland, Toowoomba, QLD 4350, Australia*

* Corresponding author: Fax: 61 2 9351 3760; E-mail: liu_hy@aeromech.usyd.edu.au
Paper published in *Composites Science and Technology*

Abstract

This paper presents an experimental study on the evaluation of bridging law for a z-pin. The relationship between the z-pin bridging force and its displacement was measured by z-pin pullout tests. The tests were carried out using three types of samples with: single small pin; 3×3 small-pins (three columns?three rows) and 3×3 big-pins. For 3×3 small-pins samples, a typical pullout curve with initial bonding, debonding and frictional sliding was obtained. A high peak value of the debonding force was reached before z-pin debonding started. After debonding was initiated, the pull-out force dropped rapidly to a lower value, the pins were then pulled out steadily against friction. However, for samples with 3x3 big-pins, it was difficult to discern the peak debonding force. The major results of this study are expected to provide a better physical understanding of the mechanics and mechanisms of z-pin bridging, aside from an efficient and accurate methodology to measure the crack-bridging law.

Keywords: Z-pin reinforcement, Pullout test, Bridging law, Interfacial debonding, Interfacial friction

1. Introduction

Through-thickness reinforcements are now widely considered as successful methods to enhance interlaminar toughness of laminated composites against delamination fracture. Since Jain and Mai developed the first micro-mechanics models for interlaminar mode I and mode II fractures in 1994 [1, 2], many research papers have been published to study the efficiency of through-thickness reinforcement and its bridging mechanisms [3-7]. Fig. 1 shows a double-cantilever-beam (DCB) specimen with z-pin reinforcement [8] showing mode I delamination. During delamination growth, a reinforcing z-pin provides a closure force against the opening crack. Simultaneously, the z-pin experiences elastic deformation, interface debonding from the laminates and, finally, frictional pullout. In the whole process, the functional relationship between the delamination crack-opening displacement and the closure force from a single pin is called the *bridging law*. The results obtained in all previous work show that the efficiency of through-thickness reinforcement is strongly dependent on the corresponding bridging law. However, a z-pin pullout is a complicated process, which is affected by many variables, for example, material properties, geometry, and interfacial parameters between the pin and the laminates. To simulate the bridging effect due to the z-pins on composite delamination, certain assumptions for the bridging law are used in all the previous numerical and theoretical studies. In Jain and Mai's models [1, 2], the interface between stitches (or z-pins) and laminates was assumed fully frictional. The bridging force due to stitching was calculated by assuming a constant frictional shear stress between the stitch and the laminates. Later, Cox presented a model of mode II delamination with a through-thickness fibre tow [3]. Here, the bridging tow was assumed to deform in shear as a rigid-perfectly plastic material. The axial sliding of the tow relative to the laminates was

frictional in nature and represented by uniform shear traction. In his numerical example, both the shear and closure tractions of the tow were given by assumed values based on observations from experiments. More recently, Liu and Mai [4] presented a theoretical model of mode I delamination of DCB with z-pinning. The bridging stress of the z-pin was calculated by a single fibre pullout model [5], which included the whole process of z-pin pullout: elastic deformation before z-pin debonding, elastic deformation and frictional sliding during debond growth and, finally, frictional sliding. Computer simulations were given for mode I delamination fracture with z-pin reinforcement. Effects of areal density, diameter, Young's modulus of z-pin and, especially, interfacial friction between the z-pin and laminates were studied in depth. Another study conducted by Liu, Yan and Mai [6] was focused on the effect of the bridging law on z-pinned mode I delamination. Here, the bridging law was simplified to either a bi-linear or tri-linear function. These functions were determined by three parameters: maximum debonding force, maximum frictional force and displacement corresponding to debonding force. Parametric studies have been presented in order to identify the dominant factors in z-pin reinforcement. Yan, Liu and Mai [7] further studied the effect of z-pinning on delamination toughness of composite laminates by using the finite element method (FEM). Different to the analytic studies, which were based on elementary beam theory, shear deformation, material orthotropy and geometric non-linearity were considered in the FEM model. The z-pin bridging law was described by a bi-linear function, which included elastic deformation and frictional sliding during z-pin pull-out. The z-pin pulling-out process was simulated by the deformation of a set of non-linear springs.

From the above discussions, it is clear that there has been much effort by researchers to try to model and quantify the effects of z-pinning on delamination growth. However, the accuracies

of their results and conclusions are very much dependent on the bridging law assumed based on the pullout mechanics of a single fibre, stitch or pin with varying degree of sophistication or complexity. Certainly, the most reliable bridging law is that determined by accurate pullout experiments. So far, there are no reported experimental details of the measured bridging law to justify the analytic models used in previous studies. This is seen as a major deficiency of current research on z-pinning and this paper aims to address this issue.

An experimental study on z-pin bridging was performed to determine directly the relationship between the bridging force and pullout displacement by the z-pin pullout test, which is shown in Fig. 2. Results were obtained for pullout of 3×3 small-pins, 3×3 big-pins and a single big-pin. We expect to obtain an in-depth physical understanding of the z-pin bridging mechanics and mechanisms. The experimental bridging law obtained can be used for future theoretical and numerical studies on through-thickness reinforcement due to z-pinning.

2. Experimental work and results

The test set-up for pullout of a 3×3 z-pins sample is shown in Fig. 2. The z-pins were made of carbon fibre (T300) reinforced BMI resin and were vertically inserted into the central areas of two carbon fibre reinforced epoxy prepregs (IMS/924) by an ultrasonic insertion machine before curing [8]. The prepreg was 40 mm long and 20 mm wide. A thermal insulated film with a thickness of 10 µm was inserted between the upper and lower laminates to avoid any adhesive bonding between them. Two T-shaped tabs (20 mm long and 15 mm wide) were glued by Araldite® Epoxy Resin Super Strength to the top and bottom surfaces of the laminates and were firmly secured in an Instron 5567 testing machine at a crosshead speed of

1 mm/min. Load-displacement curves were recorded until the pins were completely pulled out. It should be noted that in the tests, the displacements recorded by the machine also included the deformations of the two T-shaped tabs, which were attached to the sample. A separate tensile test on the tabs was done to measure their load-displacement curve. The measured displacement of the z-pinned sample was modified by taking away the deformation of the tabs from the total displacement. In all the load-displacement curves shown in this paper, deformations of the tabs have been excluded.

2.1 Results of 3?3 small-pins pull-out tests

Fig. 3 shows the load-displacement curves of 3?3 small-pins pullout tests in which the laminates were joined by three columns?three rows of pins of 0.28 mm in diameter. The pin-to-pin distance (centre-to-centre) was 3.51 mm. The sample thickness was 3 mm, which was identical to the length of the pin. Three samples were tested. It is shown in Fig. 3 that there are three stages in the whole pull-out process. In the first stage, with the applied displacement increasing, the pullout force increases rapidly until it reaches a peak value, P_{max} . Then, in the second stage, the load drops very rapidly with a very small increase of displacement. In the third stage, the load is reduced to zero with further pull-out. This phenomenon demonstrates the effects of initial bonding and interfacial friction between z-pins and laminates on the pullout process. At the beginning of the test, when the load was less than the critical value, P_{max} , the interfaces between pins and laminates were fully bonded. The pull-out forces from the pins were caused by their elastic deformation. With increasing load, interfacial debonding occurred and propagated rapidly. Hence, in the second stage, the pullout force dropped sharply. After the interface was fully debonded, the z-pins were pulled out from the

laminates. The pull-out force in the third stage was entirely caused by interfacial friction. In some cases, however, the friction can cause a minor increase of the load after the interface is fully debonded. These results have confirmed our previous assumptions on the z-pin bridging law [6].

2.2 Results of 3×3 big-pins pull-out tests

Fig. 4 shows the results of 3×3 big-pins pullout tests in which the pin diameter was 0.50 mm. The pin-to-pin distance was 3.13 mm. The crosshead speed was set at 1 mm/min. Three samples were tested. Compared to the results of small-pins tests, it was observed that the maximum debonding force of the big-pin pullout was only slightly larger than the small-pin even though the big pin diameter was about 1.8 times larger. Further, it was noted that the load-drops during debonding were not as large as those seen in the small pin tests. Except one curve, which shows an evident load-drop, the other two curves display much smaller load-drops indicating only a small difference between the maximum debonding load and the maximum frictional sliding load.

Comparisons of the axial stresses between small-pin and big-pin pullout tests are given in Fig. 5, where $\sigma_{pin,d}$ and $\sigma_{pin,f}$ are the maximum axial stress of a single pin before debonding (caused by elastic deformation) and after complete interface debonding (caused by friction), respectively. From Fig. 3 and Fig. 4, these stresses were approximately calculated by:

$$\sigma_{pin} = \frac{4\bar{P}}{9\pi d^2} \quad (1)$$

In Eq. (1), d is pin diameter and \bar{P} is average load of 3 samples. However, the value of $\sigma_{pin,f}$ of the big-pin sample was measured from one curve only as the load drop does not appear in the other two curves. It can be seen that both of these axial stresses, $\sigma_{pin,d}$ and $\sigma_{pin,f}$, of a big pin are always smaller than those of a small pin during elastic deformation and frictional pullout, respectively. During pullout of a z-pin, the load is applied to the pin end and transferred to the laminates via the interface. The equilibrium of a pin fragment (Fig. 6) requires that:

$$\tau_a(z) = -\frac{d}{4} \frac{d\sigma_{pin}(z)}{dz} \quad (2)$$

where τ_a is interfacial shear stress, which increases with applied load. Interface failure starts when τ_a exceeds its shear strength τ_s . That is, the criterion for interface debonding is:

$$\tau_a \geq \tau_s. \quad (3)$$

To understand the difference of interfacial behaviour between big-pin and small-pin tests, both sides of Eq. (3) should be considered. To examine the interfacial bonding condition, and hence τ_s , scanning electron micrographs of the fibre surfaces of both big and small pins were taken and shown in Fig. 7. It is obvious that, after pullout, the surfaces of both big and small pins are quite similar. Large quantities of the resin are plucked out from the pin during debonding. This suggests that initial chemical bonding exists between both big and small pins

with the resin of the laminates. These results therefore imply that the shear strength τ_s should be close for both pins.

To evaluate the shear stress at the big pin interface, here, our previous work on fibre pullout [5] was applied as an approximate solution. The results of the relationship between the maximum axial stress at the loaded pin-end and maximum shear stress along the pin-laminate interface were calculated and shown in Fig. 8. In these calculations, in the pinned area, the densities of z-pins were 0.5% for samples with small-pins and 2% with big-pins. Young's modulus of z-pin was taken as 170 GPa [4]. For the laminates, the moduli were calculated to be 10 GPa and 13 GPa for small-pin and big-pin samples, respectively [8, 9]. The corresponding radial thermal expansion coefficients of z-pin and laminates were $-0.3 \times 10^{-6}/^{\circ}\text{C}$ and $22 \times 10^{-6}/^{\circ}\text{C}$ [9-11]. It is obvious that, when the axial stress increases, the shear stress of big pin increases more rapidly than that of small pin. Thus, under the same applied axial stress, the interfacial shear stress in a big-pin is much higher than a small-pin. So, if their shear strengths are the same, Fig. 8 indicates that the big pin will reach this critical strength value before the small pin and hence experiences a lower interface debond stress, consistent with the experimental $\sigma_{pin,d}$ results in Fig. 5.

After debonding, the interfacial shear stress of the pin is mainly caused by frictional sliding of the pin and it can be approximated by [5]:

$$\tau_a(z) = \mu q^0 \quad (4)$$

where μ is friction coefficient and q^0 is thermal residual stress at the interface and is compressive. Since both q^0 and μ do not vary with axial position, z , the axial stress at a pin with embedded but debonded length l can be solved, that is:

$$\sigma_{pin,f} = -\frac{4l\mu q^0}{d}. \quad (5)$$

Clearly, the axial stress of the pin varies inversely with pin diameter d . Therefore, as shown in Fig. 5, the axial stress of a small pin, $\sigma_{pin,f}$, is about twice of that of a big pin.

During all the pullout tests, no pin breakage was observed. Instead, all pins were pulled out by interface failure from one single laminate. Even in the small pin tests, in which the tensile stress reached 574 MPa (Fig. 5), no pin broke before the interface failed. Hence, it could be concluded that the big pin was pulled out at a stress level much lower than its tensile strength. In z-pin reinforced laminates, high bridging stresses without pin breakage will give maximum resistance to delamination growth. Since the big pins are always pulled out at a low stress level, for a given pin areal density, small pins provide more efficient reinforcement to the laminates. This conclusion was also predicted by our previous theoretical simulation [4] and proven experimentally by Cartie [8].

2.3 Results of single pin pull-out tests

Fig. 9 shows the results of single pin pullout tests in which the pin diameter was 0.28 mm. The crosshead speed was 1 mm/min. Three samples were tested. In contrast to the 3?3 z-pin

tests, the results of 3 samples were very different. Thus, the single pin pullout tests were not as successful as the multi-pin tests. This could be caused by the poor quality of the single pin samples due to the difficulties encountered in the manufacturing process. For example, the location and orientation of the pin were very hard to control when the pin was inserted into the prepreg. In many samples, the pin was not upright and was inserted with a random angle as shown in Fig. 10(a). For comparison, in 3?3 z-pin tests, most pins remain vertical to the laminates after being pulled out, Fig. 10(b). One more serious difficulty with the single-pin tests was the alignment of the pin with the load-line. For these reasons, the single pin pullout results in Fig. 9 are not used in the bridging law analysis.

2.4 Z-pin bridging law

A single z-pin bridging law can be evaluated from the results of the above multi-pin pullout tests. As discussed in our previous work [6], a z-pin bridging law is best characterised by using a tri-linear law. Based on the experimental results shown in Figures 3 and 4 in that the precipitous load-drop for debonding is more gradual than that was given in [6], so that the bridging law evaluated from this work (Fig. 11) is determined by four parameters: maximum debonding force, P_d , maximum frictional force, P_f , and the corresponding displacements to the debonding force, δ_1 and to the maximum frictional force δ_2 . The functional relationship between the bridging force and z-pin displacement is given by:

$$P = \begin{cases} \frac{\delta}{\delta_1} P_d & (0 \leq \delta \leq \delta_1) \\ \frac{\delta_2 - \delta}{\delta_2 - \delta_1} P_d + \frac{\delta - \delta_1}{\delta_2 - \delta_1} P_f & (\delta_1 \leq \delta \leq \delta_2) \\ P_f + \frac{\delta_2 - \delta}{h - \delta_2} P_f & (\delta_2 < \delta \leq h) \end{cases} \quad (6)$$

From 3?3 small-pins pullout (Fig. 3) tests, the average maximum debonding load and the average maximum friction load of three samples are 318 N and 142 N, respectively. So the corresponding P_d and P_f in a single pin can be calculated as, $P_d=35.3$ N and $P_f=15.7$ N. The average displacements δ_1 and δ_2 were 0.037 mm and 0.170 mm, respectively. From the 3?3 big-pins pullout (Fig. 4) tests, the four parameters are measured as: $P_d=38.3$ N, $P_f=28.2$ N, $\delta_1=0.130$ mm and $\delta_2=0.231$ mm. Since the load drop of debonding only occurs in one big-pin sample, the data of P_f and δ_2 of big-pin tests given above were measured from one curve only. Other two parameters of big-pin tests, P_d and δ_1 were evaluated by averaging the maximum loads and the corresponding displacements among three samples. As we analysed in [6], if there is no debonding load-drop, the bridging law will be simplified to a bi-linear function determined by two parameters: maximum load and the corresponding displacement. Hence, Eq. (6) will be given by the first and third equations with $P_d (=P_f)$ and $\delta_1 (= \delta_2)$.

In the analyses of z-pinned DCB delamination [1, 4, 6, 7], the bridging law is always given for one-half of the pin because of the symmetry of the DCB geometry. In Fig. 11, h is half-pin length and δ_1 is the maximum displacement of a half-pin before debonding. In the tests, the displacement was measured for the full-pin length. Therefore, δ_1 in Fig. 3 and Fig. 4

should be halved corresponding to the maximum load, P_d . These values are 0.0185 mm and 0.065 mm for the small-pin and big-pin, respectively.

In an ideal z-pin pullout test, the applied load should be equally supported by all bridging pins. Hence, all pins should be pulled out equally from both upper and lower laminates since the interfacial conditions along all pins should be identical. Thus, the total pullout distance should be the full-pin length equal to 3 mm. However, this perfect situation is very difficult to achieve. Clearly, in Fig. 3 and Fig. 4, the maximum pullout distance is always less than the pin length. Post-test observations showed that all z-pins were almost always pulled out from one side. This confirms possible differences of interfacial properties from pin to pin even in one sample. When debonding started in one side, the pin began to slide resulting in a load-drop. The reduced external load would not be sufficient to initiate debonding and pullout of the pin from the other side. So, in all cases, the z-pins were pulled out from one side. Supporting evidence is provided in Fig. 3 and Fig. 4, wherein the displacements at complete pullout of the z-pins are about 1.5 to 2 mm, being approximately one-half the thickness of the samples and z-pins. However, it is more accurate to measure the pullout lengths of the pins after testing. Thus, 16 pins from eight samples were measured using a microscope (WILD Heerbrugg[®]) and the lengths varied from 1.3 to 1.7 mm, which were close to the half-pin length of 1.5 mm. Hence, it is verified that the z-pins were mainly pulled out from one side of the samples.

In the z-pin bridging law, Eq (6), h is the maximum pullout distance, which is the half-length of the pin. However, it is seen, in Fig. 3 and Fig. 4, that in some cases, the pullout distance is larger than h . It may be caused by inaccurate locations of the pins, which should be inserted

ideally in the central area of the test samples. But this is not always achievable, especially for the single-pin insertion process. The inaccuracy of pin location will give rise to non-uniform load distribution on the pins and eccentric loading may also cause bending of the pins. Indeed in the tests, it was observed that the two laminates were not always parallel to each other but with a tiny relative rotation between them as they were pulled apart. These problems must be realised and rectified in the multi-pin pullout test methodology if accurate bridging laws are to be determined.

3. Conclusions

Z-pin pullout tests were carried out to study the z-pin bridging mechanism and mechanics in mode I delamination. Load-displacement curves showing initial elastic bonding, unstable debonding and frictional sliding were obtained for 3?3 multi-pin and single-pin samples. These results confirmed our assumptions of the z-pin bridging law and computer simulation studies in our previous work [4, 6, 7]. From the present pullout tests, we can draw the following conclusions:

- (i) With the same areal density, small pins provide more efficient reinforcement than big pins.
- (ii) Since single pin orientation is difficult to control during insertion and load-displacement alignment almost impossible to obtain in single-pin pullout tests, multi-pin tests are preferred as they will provide more reliable and accurate results.
- (iii) In big-pin pullout tests, the load-drop caused by interfacial debonding is not as evident as in the small pin tests because there is only a small difference between the initial debonding load and the initial frictional sliding load.

Acknowledgements

The authors would like to thank the Australian Research Council (ARC) for the continuing support of this project. Y-W Mai and H-Y Liu are supported by an Australian Federation Fellowship and an Australian Research Fellowship, respectively, funded by the ARC and tenable at the University of Sydney. Professor Ivana Partridge and Dr Denis Cartié of Cranfield University kindly provided all the z-pinned composite samples for the pullout tests. Their helpful discussions and constructive input during the course of the project are much appreciated.

References

1. Jain LK, Mai Y-W. On the Effect of Stitching on Mode I Delamination Toughness of Laminated Composites. *Composites Science and Technology* 1994;51:331-345.
2. Jain LK, Mai Y-W. Analysis of Stitched Laminated ENF Specimens for Interlaminar Mode-II Fracture Toughness. *International Journal of Fracture* 1994;68:219-244.
3. Cox BN. A Constitutive Model for Through-Thickness Reinforcement Bridging a Delamination Crack. *Advanced Composites Letters* 1999;8(5):249-256.
4. Liu H-Y, Mai Y-W. Effects of Z-pin Reinforcement on Interlaminar Mode I Delamination. In: *Proceedings of the 13th International Conference on Composite Materials, ICCM13; Beijing, China 2001.*
5. Liu H-Y, Zhang X, Mai Y-W, Diao X-X. On Steady-state Fibre Pull-out Part II: Computer Simulation. *Composites Science and Technology* 1999;59:2191-2199.

6. Liu H-Y, Yan W, Mai Y-W. Z-Fibre Bridging Stress in Composite Delamination. In: *Fracture of Polymers, Composites and Adhesives II,ESIS Publication 32*. Editors: B. R. K. Blackman, A. Pavan and J. G. Williams, 2003, pp. 491-502.
7. Yan W, Liu H-Y, Mai Y-W. Numerical Study on the Mode I Delamination Toughness of Z-Pinned Laminates. *Composites Science and Technology* 2003;63:1481-1493.
8. Cartie DDR. Effect of Z-FibreTM on the Delamination Behaviour Carbon Fibre/Epoxy Laminates. PhD Thesis, Cranfield University, 2000.
9. Ashbee K. *Fundamental Principles of Fibre Reinforced Composites* 2nd ed., Technomic Publishing Co., Inc, USA, 1993.
10. Tan L-S. *Polymer Data Handbook*. Oxford University Press, Inc., 1999.
11. Cheremisinoff, NP. *Handbook of Ceramics and Composites, Vol. 2*. Marcel Dekker, New York. 1992.

Figure Captions

Fig. 1. Composite delamination with z-pins pullout [8].

Fig. 2. Illustration of experimental configuration for 3?3 z-pins pull-out tests.

Fig. 3. Load-displacement curves of 3×3 small-pins pullout with crosshead speed, $v_0=1$ mm/min.

Fig. 4. Load-displacement curves of 3×3 big-pins pullout with crosshead speed $v_0= 1$ mm/min.

Fig. 5. Maximum tensile stresses of a small pin and a big pin before interface debonding and during frictional pullout.

Fig. 6. Illustration of equilibrium between axial stress and interfacial shear stress of a pin fragment.

Fig. 7. SEM photos of (a) small pin and (b) big pin after pullout.

Fig. 8. Relationship between the axial stress and interfacial shear stress in a single pin.

Fig. 9. Load-displacement curves of single small pin pull-out with a crosshead speed $v_0= 1$ mm/min.

Fig. 10. (a) A single pin; and (b) 3×3 pins after pullout tests.

Fig. 11. A simplified bridging law in z-pinned DCB mode I delamination analysis, in which $P_d=35.3$ N, $P_f=15.7$ N, $\delta_1=0.0185$ mm and $\delta_2=0.170$ mm for small-pin sample and $P_d=38.3$ N, $P_f=28.2$ N, $\delta_1=0.065$ mm and $\delta_2=0.231$ mm for big-pin sample.

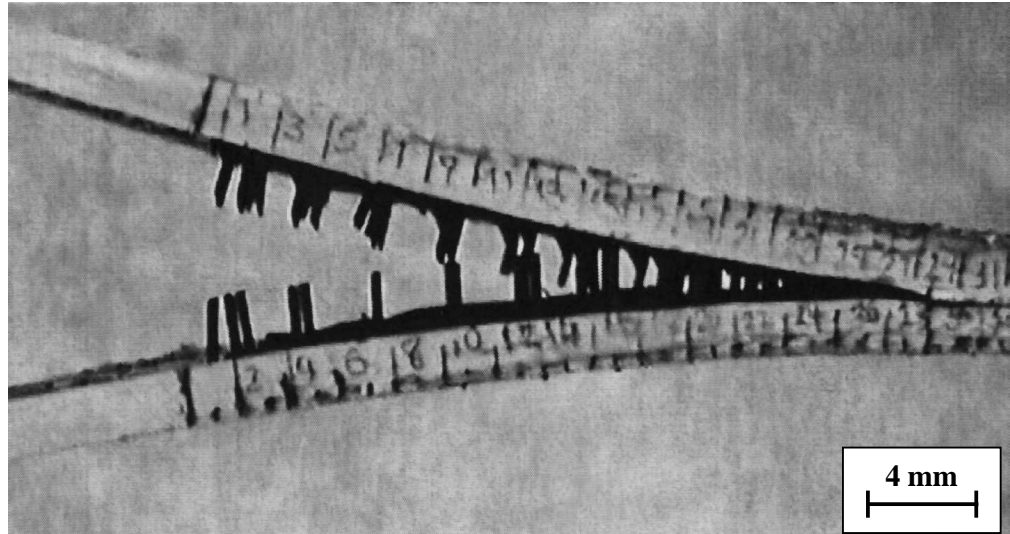


Fig. 1. Dai, Yan, Liu and Mai

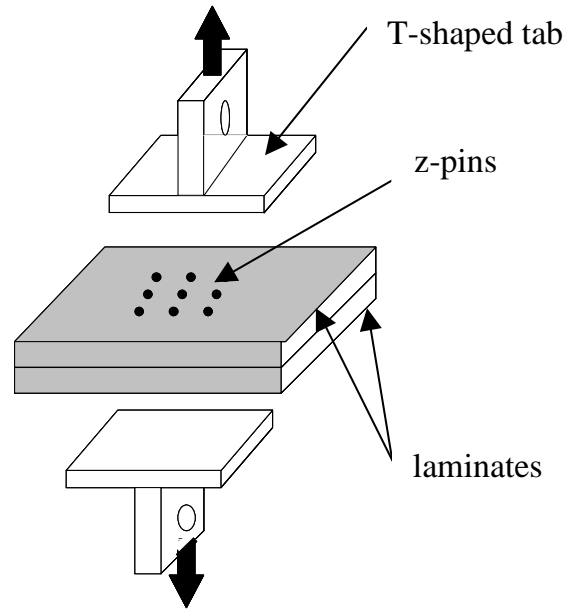


Fig. 2. Dai, Yan, Liu and Mai

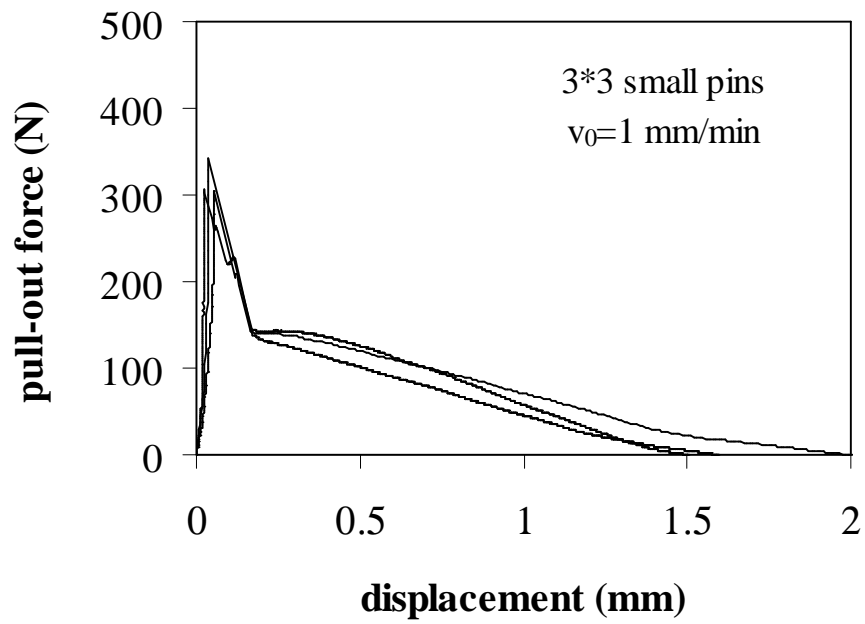


Fig. 3. Dai, Yan, Liu and Mai

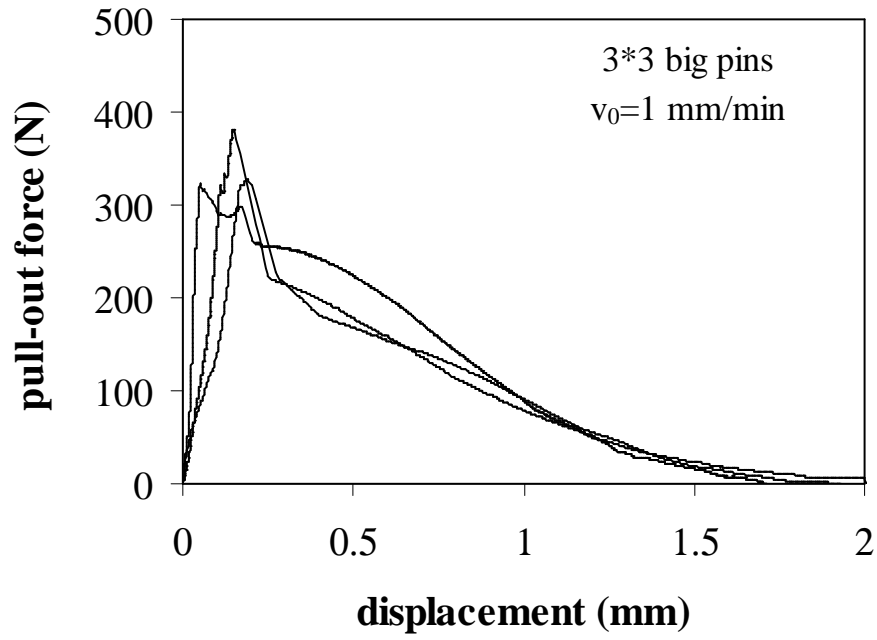


Fig. 4. Dai, Yan, Liu and Mai

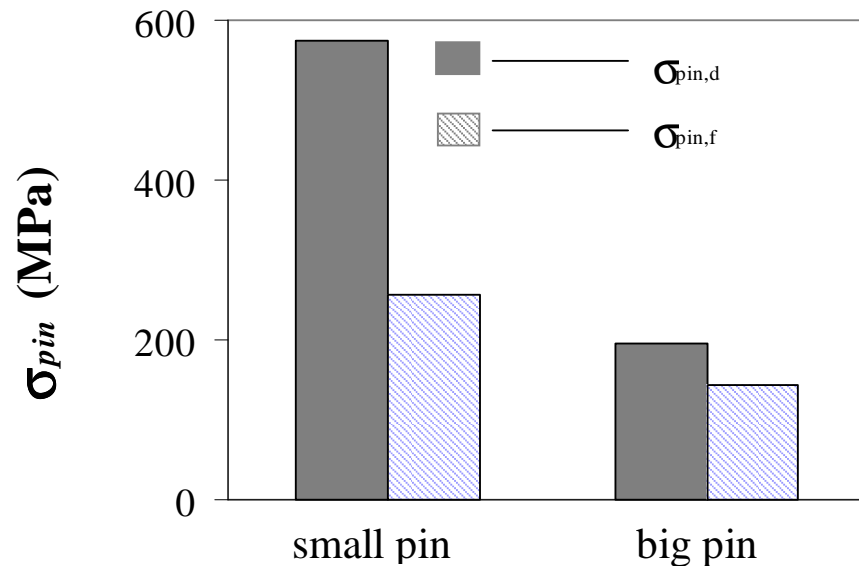


Fig. 5. Dai, Yan, Liu and Mai

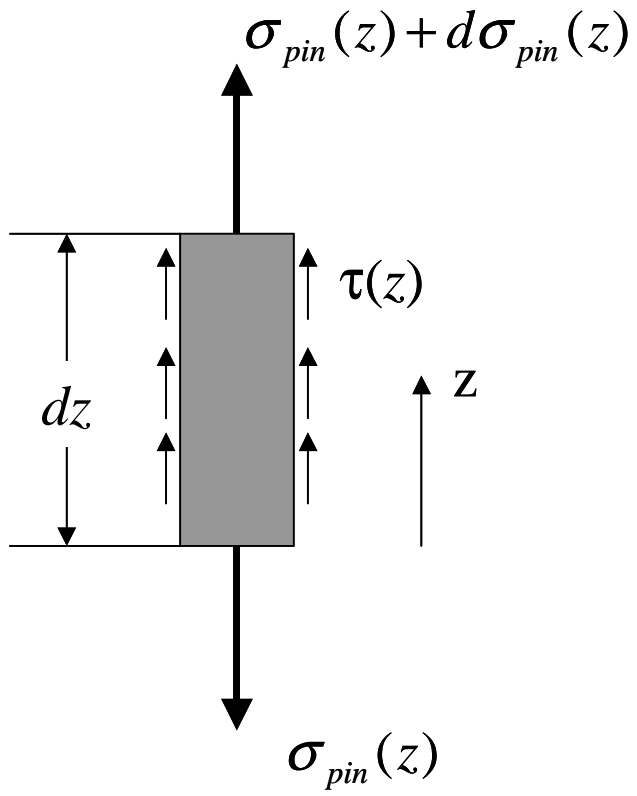
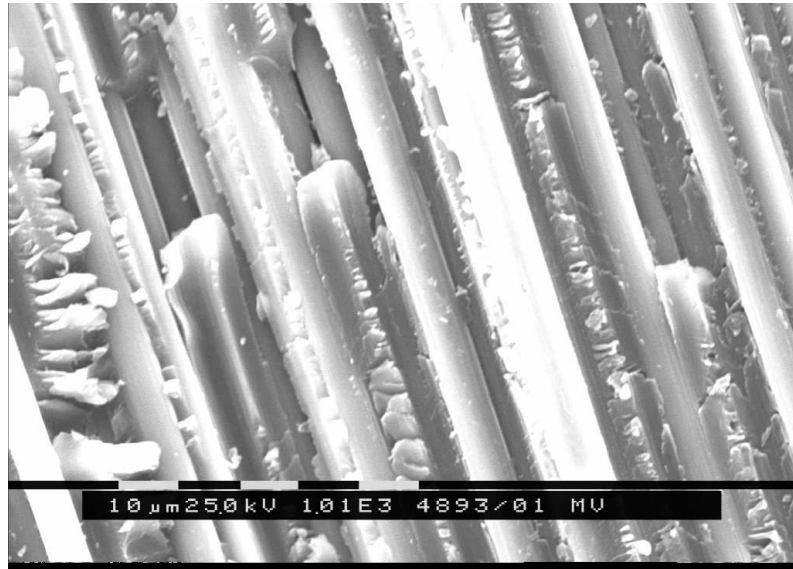
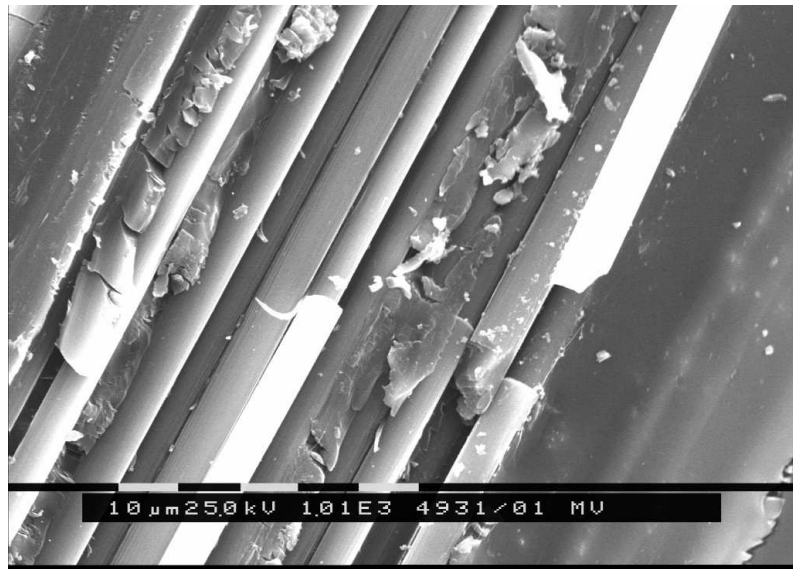


Fig. 6. Dai, Yan, Liu and Mai



(a)



(b)

Fig. 7. Dai, Yan, Liu and Mai

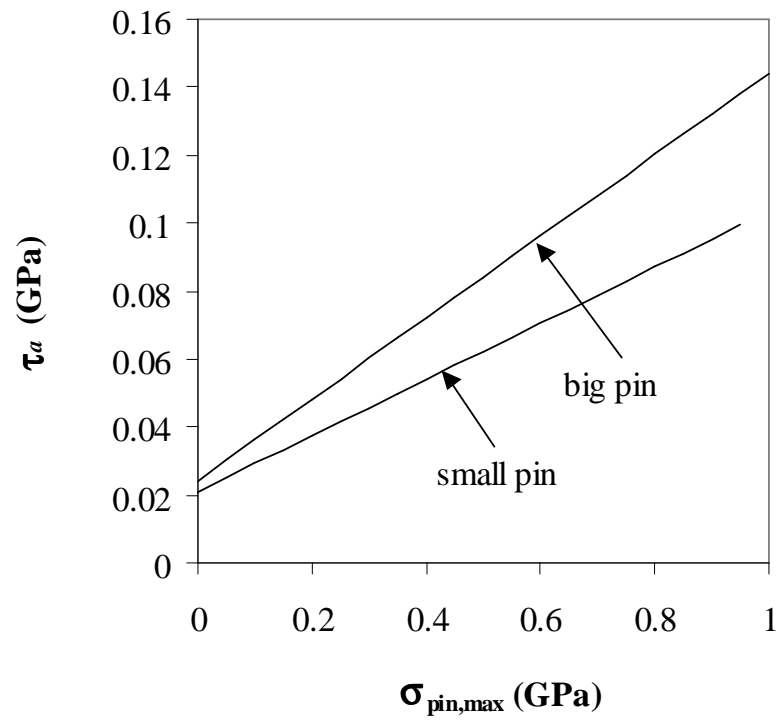


Fig. 8. Dai, Yan, Liu and Mai

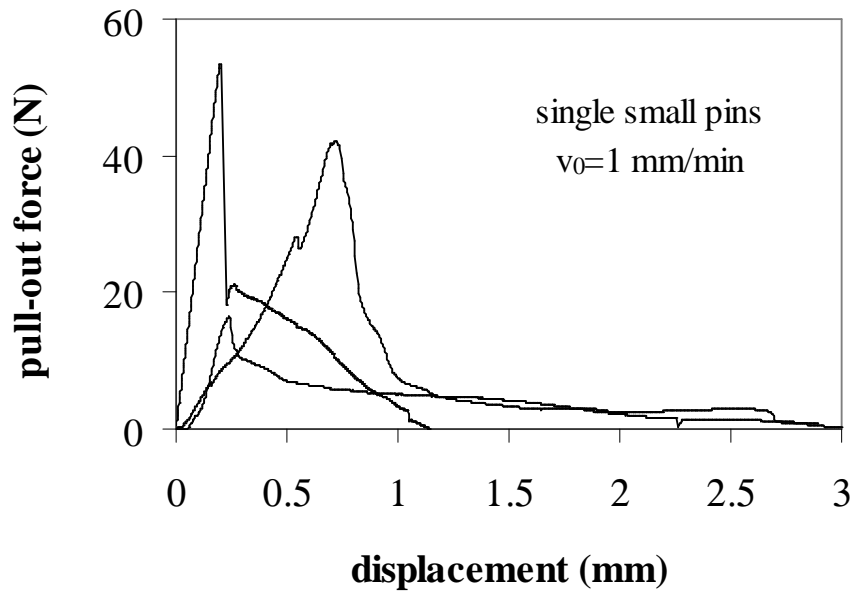
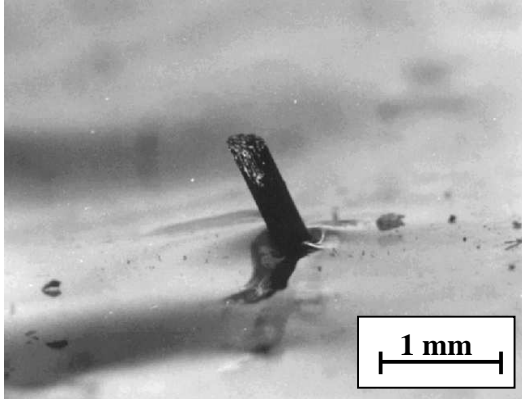
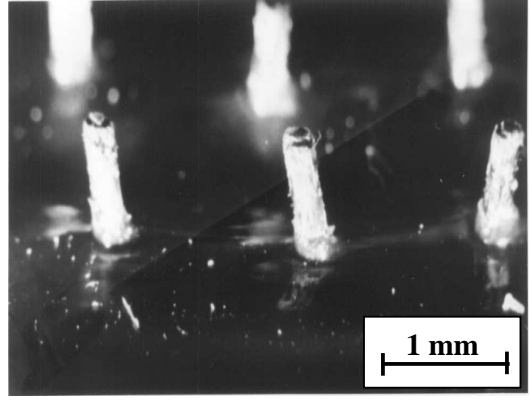


Fig. 9. Dai, Yan, Liu and Mai



(a)



(b)

Fig. 10. Dai, Yan, Liu and Mai

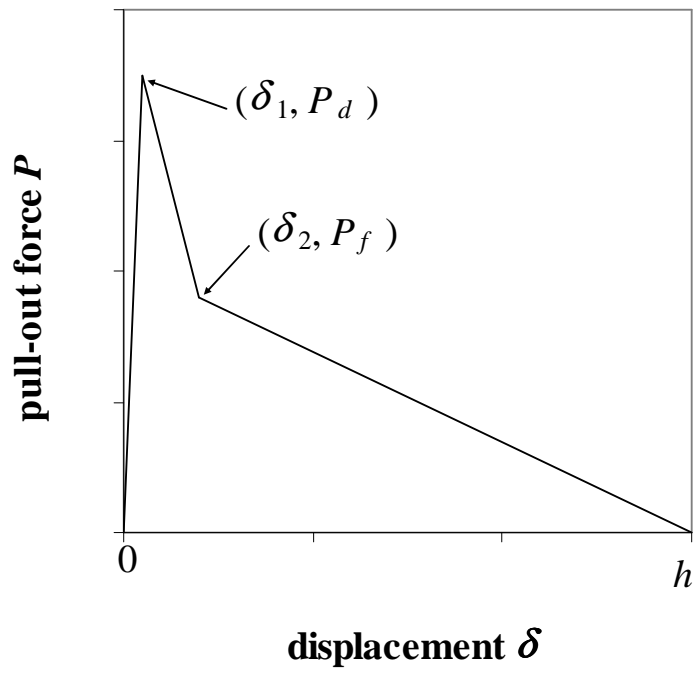


Fig. 11. Dai, Yan, Liu and Mai